Skyrmion Lattice Order Controlled by Confinement Geometry

Raphael Gruber[1], Jan Rothörl[1], Simon M. Fröhlich[1], Maarten A. Brems[1], Fabian Kammerbauer[1], Maria-Andromachi Syskaki[1,2], Elizabeth M. Jefremovas[1], Sachin Krishnia[1], Asle Sudbø[3], Peter Virnau[1], Mathias Kläui[1,3*]

1. Institute of Physics, Johannes Gutenberg-Universität Mainz, Staudingerweg 7, 55128 Mainz, Germany.
2. Singulus Technologies AG, Hanauer Landstraße 103, 63796 Kahl am Main, Germany.
3. Center for Quantum Spintronics, Department of Physics, Norwegian University of Science and Technology, 7491 Trondheim, Norway.

*Email: klaeui@uni-mainz.de

Abstract

Magnetic skyrmions forming two-dimensional (2D) lattices provide a versatile platform for investigating phase transitions predicted by Kosterlitz-Thouless-Halperin-Nelson-Young (KTHNY) theory. While 2D melting in skyrmion systems has been demonstrated, achieving controlled ordering in skyrmion lattices remains challenging due to pinning effects from a non-uniform energy landscape, which often results in polycrystalline structures. Skyrmions in thin films, however, offer thermal diffusion with high tunability and can be directly imaged via Kerr microscopy, enabling real-time observation of their dynamics. To regulate lattice order in such flexible systems, we introduce geometric confinements of varying shapes. Combining Kerr microscopy experiments with Thiele model simulations, we demonstrate that confinement geometry critically influences lattice order. Specifically, hexagonal confinements commensurate with the skyrmion lattice stabilize monodomain hexagonal ordering, while incommensurate geometries induce domain formation and reduce overall order. Understanding these boundary-driven effects is essential for advancing the study of 2D phase behavior and for the design of skyrmion-based spintronic applications, ranging from memory devices to unconventional computing architectures.

Magnetic skyrmions are topologically non-trivial chiral spin textures that exhibit quasi-particle behavior[1–3]. Their small size, stability, and dynamic properties make them highly promising for energy-efficient spintronic applications ranging from data storage[4] to sensing[5] and unconventional computing – where so far single skyrmions have been used[6–9]. For enhanced complexity however, arrangements of multiple skyrmions can be envisaged[10]. Beyond their technological significance for data processing, systems of dense skyrmion arrangements give rise to intriguing phenomena such as skyrmion drag[11]. And even denser lattice arrangements of skyrmions provide an ideal platform for exploring fundamental two-dimensional (2D) ordering phenomena[12–15] as quasi-long-range order (QLRO) can arise[12–16].

Skyrmion quasi-particles can exhibit thermally activated Brownian dynamics[17–19] and offer on-the-fly tunability of both their size and their diffusivity[18,20–22]. This versatility allows to investigate lattice phenomena beyond current observations and is a key advantage of skyrmions over other 2D systems like colloids or superconducting vortices. In particular, the tunability can be exploited to drive and observe 2D phase transitions[15] as described in Kosterlitz-Thouless-Halperin-Nelson-Young (KTHNY) theory[23–27]. These 2D phase transitions differ fundamentally from behavior in other dimensions, particularly from 3D. In particular, KTHNY theory describes the existence of a hexatic phase with only orientational QLRO between the solid phase (with translational QLRO) and the isotropic liquid (no QLRO)[25–27]. Eventually, these ordered lattice can even allow data transport by exploiting shock waves or the dynamics of topological lattice defects, which can move orders of magnitude faster than skyrmions[15,16]. Consequently, 2D phase transitions have attracted significant fundamental research interest for decades, both in theory and experiments[12,15,23–29].

In experimental skyrmion lattices, the key challenge in realizing QLRO is the underlying non-uniform energy landscape caused by material inhomogeneities[13–15,30]. The non-flat energy landscape describes a continuously varying potential with attractive as well as repulsive sites[18,31] – often commonly referred to as pinning effects. It causes quenched disorder, topological lattice defects and polycrystallinity, together breaking the QLRO of the lattice[13,30]. The local order is quantified by the orientational order parameter

$$\psi_6(\mathbf{r}_j) = \frac{1}{n}\sum_{k=1}^{n} e^{-i6\theta_{jk}} \tag{1}$$

for every skyrmion j at position $\mathbf{r}_j$ and with n nearest neighbors at positions $\mathbf{r}_k$ (k=1…n); where θ_{jk} denotes the angle between the horizontal axis (arbitrarily chosen) and the vector $\mathbf{r}_k$-$\mathbf{r}_j$ connecting the neighbor pair j and k[25]. The Euler angle of the complex value of ψ_6 directly determines the local orientation $\alpha(\mathbf{r}_j)=\arg[\psi_6(\mathbf{r}_j)]/6$ of the lattice for every skyrmion. Regions of similar orientation α form a lattice domain. In a polycrystalline lattice, multiple lattice domains exist with different orientation of each domain. The domains are separated by boundaries at which α changes abruptly. These domain boundaries have been shown to be effectively pinned due to a non-flat energy landscape[30]. Thus, the lattice domains and their orientation appear pinned by the sample-specific energy landscape, imposing uncontrolled boundary conditions which are likely to be incommensurate with the ideal hexagonal skyrmion lattice.

To overcome this limitation, in this work, we artificially tune the boundary conditions by confining the skyrmion lattices inside different geometrical shapes. We find that commensurate shapes enhance the lattice order compared to an unconfined lattice, while the order is suppressed by incommensurate shapes. The results are consistent for Kerr microscopy experiments as well as Thiele model simulations[31–33].

We stabilize a polycrystalline skyrmion lattice close to room temperature (335 K) in a Ta(5 nm)/$Co_{20}Fe_{60}B_{20}$(0.9 nm)/Ta(0.07 nm)/MgO(2 nm)/Ta(5 nm) magnetic thin film multilayer

stack with various confinement patterns (see supplementary material with Fig. S1 for details). The skyrmions are imaged in real-time (16 fps) and -space by using a commercially available Kerr microscope by *evico magnetics GmbH* using the polar magneto-optical Kerr effect. In Fig. 1a, we show a Kerr image of a skyrmion lattice in a hexagonal confinement. We use the *trackpy*[34] Python package to track the skyrmions and a Voronoi tessellation[35] to determine the lattice neighbors as well as the local order. After nucleation, the lattice evolves in time. In Fig. 1b, we color the local lattice orientation α for different snapshots of one video. While several small lattice domains are present in the beginning, the whole lattice aligns with the hexagonal confinement within minutes. The growth of the lattice domains is accelerated by an oscillating magnetic out-of-plane (OOP) field[20]. The hexagonal confinement is commensurate with the hexagonal skyrmion lattice structure and therefore allows stabilization of QLRO on this finite length scale[15].

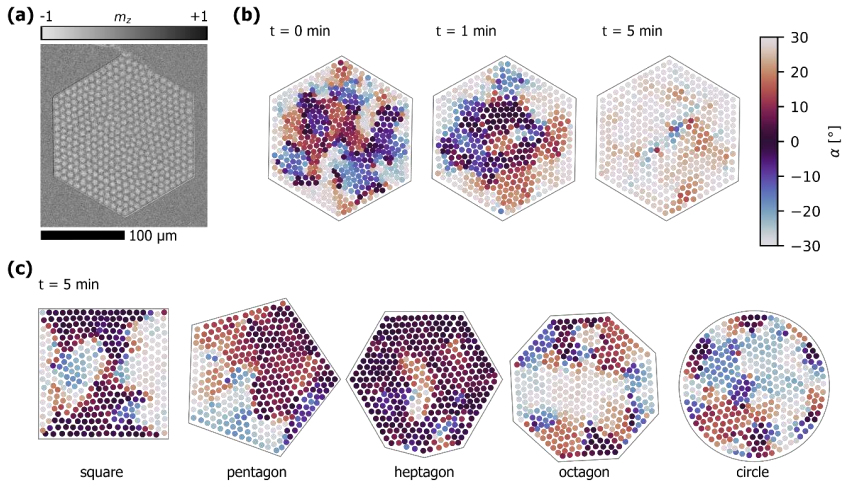

Fig. 1: (a) Polar Kerr microscopy image of a skyrmion lattice in a hexagonal confinement. **(b)** After nucleation, the skyrmion lattice arranges into hexagonal order on time scales of minutes within the commensurate hexagonal confinement, illustrated by the color-coded lattice orientation α per skyrmion for t=0,1,5 min after nucleation. Due to the six-fold symmetry of the hexagonal lattice, the color map of α is cyclic. **(c)** In different geometries, the incommensurate edges anchor different lattice domains, suppressing hexagonal order even after t=5 min.

As a comparison, in Fig. 1c, we present skyrmion lattices confined in different, incommensurate geometric shapes. All confinements are patterned on the same sample piece and have nominally the same area as the hexagon. Furthermore, all shapes are regular, except for the heptagon, which is a hexagon with an additional kink. In all geometries, the lattice locally aligns with the confinement edges and is therefore frustrated for the incommensurate shapes. Consequently, distinct lattice orientations are anchored at the boundary and enforce the occurrence of domain boundaries between each other[30]. While for the pentagon, every corner induces only a slight distortion, in total causing one domain boundary through the center, the many orientations around the octagon and the circle lead to much smaller areas of similar orientation. The distortions caused by the subtle irregularity of the heptagon can range from only slight misalignment of the outermost 2-3 skyrmion layers to even significant distortions far inside the lattice. In principle, a regular triangle would also be commensurate with the hexagonal lattice and

therefore expected to enhance lattice order. However, edge effects may play a role in comparison to the hexagonal shape as the distances of every skyrmions to the edges are distributed differently.

To compare the lattice order in the different confinements quantitatively, we calculate the average local order $\Psi_6=\langle|\psi_6|\rangle$ as well as $\chi_6=|\langle\psi_6\rangle|$ in Fig. 2. For both parameters, higher values indicate better ordering. We furthermore compare the results to videos of a continuous sample of millimeter extension, where no confinements are patterned and around 3500 skyrmions are nucleated in the field of view. We find that the ordering is enhanced in the commensurate hexagon and suppressed for the incommensurate shapes. Thereby, χ_6 reveals more drastic differences as it globally averages over α, thus providing more long-range information but being significantly affected by changes of α, that occur for instance at domain boundaries.

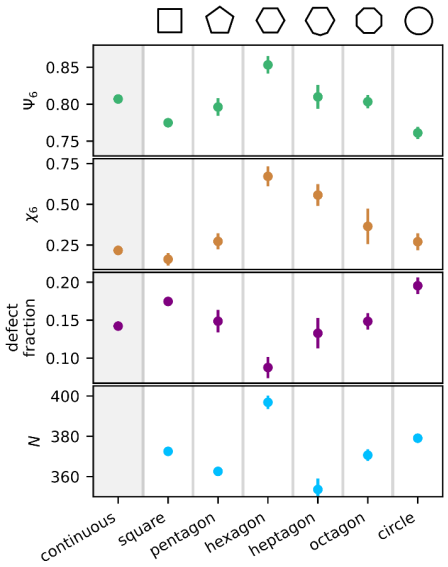

Fig. 2: Order parameters Ψ_6 and χ_6, fraction of lattice defects and number of skyrmions N compared for different confinement geometries and a lattice in an unpatterned, continuous film (N>3000) for reference. Data points are the average values from the last minute (4 min < t < 5 min) of three independent videos. While the commensurate hexagonal confinement enhances the lattice order, incommensurate geometries suppress order with respect to the continuous case. From the mean values of the three different nucleations, we calculate the standard error of the mean as the error bar.

Correspondingly, the fraction of skyrmions being a topological lattice defect (i.e., $n\neq6$ lattice neighbors) increases for reduced ordering. The topological defects emerge as an intrinsic property of 2D lattices mediating their phase behavior[23–27], but also at domain boundaries or pinning sites. Even though a similar amount of N=510±20 skyrmions is created per nucleation (at t=0) in every geometry, we notice a clear difference in the annihilation rate for the different shapes: Skyrmion annihilation is less pronounced for the hexagon being commensurate with the hexagonal lattice, resulting in around N=395±5 skyrmions remaining at t=5 min; which is particularly close to the centered hexagonal number 401. In the incommensurate shapes however, the different lattice

domains and domain boundaries cause space conflicts, which lead to skyrmion annihilations and result in only N=365±15 at t=5 min. In the continuous reference area, N=2620±15 skyrmions are left after 5 min, all of them are included to calculate the plotted order parameters. The time evolution of all shown parameters is presented in Fig. S2 in the supplementary material.

Our results demonstrate that confinement geometries play a critical role in stabilizing lattice order. By carefully designing the boundary conditions, however, the degree of order in skyrmion lattices can be effectively controlled – while the finite size itself has been shown only have a minor effect on the 2D phase behavior[15]. To understand the commensurability effect, we next perform Thiele model simulations[31–33] using confinements of different geometry.

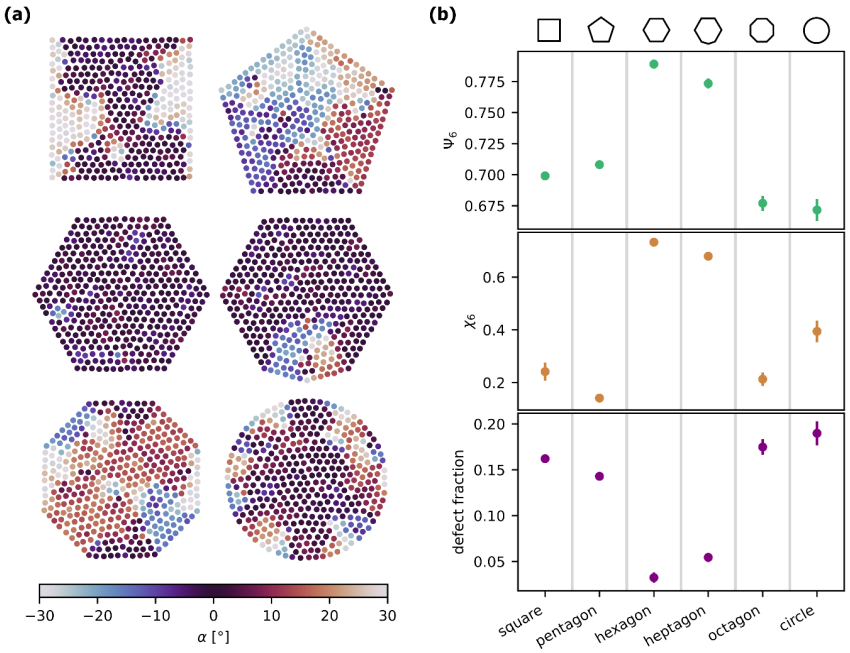

Fig. 3: (a) Local orientation α for simulated skyrmion lattices (N=400) in confinement, reproducing the alignment of lattice domains with the confinement edges and leading to multidomain states in incommensurate geometries. **(b)** The ordering parameters Ψ_6 and χ_6 as well as the fraction of lattice defects behave similar to the experiment: the lattice order is significantly enhanced in the commensurate hexagon and the closely related heptagon. Data points are averages over 3×1000 snapshots, where the error bar is calculated as the standard error of the mean from the three independent data sets.

In the simulations, we employ a purely repulsive interaction potential of the form r^{-8}, which has been demonstrated to describe our experimental skyrmion system well[15,30,36] (see supplementary material with Fig. S3 for details). We find that the simulated particles align with the edges of the confinements as in the experiment and anchor differently oriented domains. We show examples of snapshots for every shape in Fig. 3a. The extent of the single domains varies between the 1000 snapshots of three different equilibration sequences of the system. However, the average ordering

(reflected by Ψ_6, χ_6, and the fraction of lattice defects) is consistent as presented in Fig. 3b. Especially, we reproduce the experimental result that the lattice order is suppressed in incommensurate geometric confinements. The error bars (calculated as standard error of the mean from the three equilibration sequences) are only visible for the incommensurate geometries as different lattice domains are forced to coexist but can have varying extent and distribution from snapshot to snapshot. For example, the distortion induced in the heptagon affects the 8 outermost skyrmion layers in Fig. 3a. However, in some equilibration sequences, it may only affect 2-3 layers but can – in analogy to the experiment – even reach the center of the geometry in other sequences, depending on the specific configuration. In contrast, the distribution of domains in the experiment is additionally influenced by the energy landscape which yields certain preferences for domain orientations and domain boundaries[30].

In conclusion, we demonstrate in both Kerr microscopy experiments and molecular dynamics simulations that the order of a confined magnetic skyrmion lattice can be tuned as it strongly depends on the confinement geometry. While a hexagonal confinement is commensurate with the hexagonal skyrmion lattice structure and stabilizes the lattice order, incommensurate geometries suppress order and differently oriented lattice domains form along the edges. In magnetic thin films, lattice domains are typically pinned in a similar way by the non-flat energy landscape[30]. Therefore, understanding those boundary effects is key to study 2D phase behavior with skyrmions on larger scales. Magnetic skyrmions are of special interest for investigating 2D phase behavior as their real-time accessibility in Kerr microscopy can allow one to investigate key open questions like the dynamics of topological defects[15] and their interaction potential – even in the presence of a Magnus force. Understanding and controlling the dynamics of densely packed skyrmions in a confined geometry[6,7,19] also plays a key role for realizing low-power non-conventional computing applications[5–7].

Supplementary Material

See the supplementary material for a detailed description of the experimental and simulation setups.

Acknowledgements

This work was funded by the Deutsche Forschungsgemeinschaft (DFG, German Research Foundation) - SPP 2137 (project #403502522), TRR 173/2 Spin+X (projects A01, A12 and B02). The authors acknowledge funding from TopDyn. This project has received funding from the European Research Council (ERC) under the European Union's Horizon 2020 research and innovation program (Grant No. 856538, project "3D MAGiC") and under the Marie Skłodowska-Curie grant agreements No. 860060 ("MagnEFi") and No. 101119608 ("TOPOCOM"). The authors gratefully acknowledge the computing time granted on the supercomputer MOGON II and III at Johannes Gutenberg University Mainz as part of NHR South-West. M.A.B. was supported by a doctoral scholarship of the Studienstiftung des deutschen Volkes. E.M.J. acknowledges the Alexander von Humboldt Postdoctoral Fellowship. A.S. and M.K acknowledge support from the Norwegian Research Council through Grant No. 262633, Center of Excellence on Quantum Spintronics (QuSpin). A. S. also acknowledges support from Norwegian Research Council through Grant No. 323766.

Author Declaration Section

Conflict of Interest

The authors have no conflicts to disclose.

Author Contributions

R.G. performed the Kerr microscopy measurements and experimental data analysis. S.M.F., J.R. and M.A.B. conducted the MD simulations; R.G., J.R, S.M.F and M.A.B analyzed the simulation data. F.K. and M.A.S. optimized and fabricated the multilayer stack. R.G. prepared the manuscript with the help of J.R., M.A.B., E.M.J. and S.K.; A.S., P.V. and M.K. guided and supervised the work. All authors have commented on the manuscript.

Data Availability Statement

The data that support the findings of this study are available on Zenodo under https://doi.org/10.5281/zenodo.17406257[37] [will be activated after acceptance, preview under https://zenodo.org/records/17406257?preview=1&token=eyJhbGciOiJIUzUxMiJ9.eyJpZCI6IjBkYWQ3NDMwLTk0NTUtNDNkYy05ZjU4LTJjNDgwMjAwMTUwZSIsImRhdGEiOnt9LCJyYW5kb20iOiI3ZTNkMzdjZWU0OGI3ZDk3YzI3NjIwNjFmNDE1YTRiNCJ9.AEbT5glS_-4UNo_7Ra1FwJf9pGzDMoIwj2G7yEvL-mImhzb-15QjhNANylaBZBKhx2np4Ayg_dyozwZCUnz7YA]..

References

[1] A. Bogdanov, and A. Hubert, "Thermodynamically stable magnetic vortex states in magnetic crystals," J. Magn. Magn. Mater. **138**(3), 255–269 (1994).
[2] S. Mühlbauer, B. Binz, F. Jonietz, C. Pfleiderer, A. Rosch, A. Neubauer, R. Georgii, and P. Böni, "Skyrmion Lattice in a Chiral Magnet," Science **323**(5916), 915–919 (2009).
[3] K. Everschor-Sitte, J. Masell, R.M. Reeve, and M. Kläui, "Perspective: Magnetic skyrmions—Overview of recent progress in an active research field," J. Appl. Phys. **124**(24), 240901 (2018).
[4] A. Fert, V. Cros, and J. Sampaio, "Skyrmions on the track," Nat. Nanotechnol. **8**(3), 152–156 (2013).
[5] K. Leutner, T.B. Winkler, R. Gruber, R. Frömter, J. Güttinger, H. Fangohr, and M. Kläui, "Skyrmion automotion and readout in confined counter-sensor device geometries," Phys. Rev. Appl. **20**(6), 064021 (2023).
[6] K. Raab, M.A. Brems, G. Beneke, T. Dohi, J. Rothörl, F. Kammerbauer, J.H. Mentink, and M. Kläui, "Brownian reservoir computing realized using geometrically confined skyrmion dynamics," Nat. Commun. **13**(1), 6982 (2022).
[7] G. Beneke, T.B. Winkler, K. Raab, M.A. Brems, F. Kammerbauer, P. Gerhards, K. Knobloch, S. Krishnia, J.H. Mentink, and M. Kläui, "Gesture recognition with Brownian reservoir computing using geometrically confined skyrmion dynamics," Nat. Commun. **15**(1), 8103 (2024).
[8] O. Lee, R. Msiska, M.A. Brems, M. Kläui, H. Kurebayashi, and K. Everschor-Sitte, "Perspective on unconventional computing using magnetic skyrmions," Appl. Phys. Lett. **122**(26), 260501 (2023).
[9] M.A. Brems, M. Kläui, and P. Virnau, "Circuits and excitations to enable Brownian token-based computing with skyrmions," Appl. Phys. Lett. **119**(13), 132405 (2021).
[10] T.B. Winkler, J. Rothörl, M.A. Brems, G. Beneke, H. Fangohr, and M. Kläui, "Coarse-graining collective skyrmion dynamics in confined geometries," Appl. Phys. Lett. **124**(2), 022403 (2024).
[11] C. Reichhardt, "Dynamics and nonmonotonic drag for individually driven skyrmions," Phys. Rev. B **104**(6), (2021).

[12] P. Huang, T. Schönenberger, M. Cantoni, L. Heinen, A. Magrez, A. Rosch, F. Carbone, and H.M. Rønnow, "Melting of a skyrmion lattice to a skyrmion liquid via a hexatic phase," Nat. Nanotechnol. **15**(9), 761–767 (2020).
[13] J. Zázvorka, F. Dittrich, Y. Ge, N. Kerber, K. Raab, T. Winkler, K. Litzius, M. Veis, P. Virnau, and M. Kläui, "Skyrmion Lattice Phases in Thin Film Multilayer," Adv. Func. Mater. **30**(46), 2004037 (2020).
[14] P. Meisenheimer, H. Zhang, D. Raftrey, X. Chen, Y.-T. Shao, Y.-T. Chan, R. Yalisove, R. Chen, J. Yao, M.C. Scott, W. Wu, D.A. Muller, P. Fischer, R.J. Birgeneau, and R. Ramesh, "Ordering of room-temperature magnetic skyrmions in a polar van der Waals magnet," Nat. Commun. **14**(1), 3744 (2023).
[15] R. Gruber, J. Rothörl, S.M. Fröhlich, M.A. Brems, F. Kammerbauer, M.-A. Syskaki, E.M. Jefremovas, S. Krishnia, A. Sudbø, P. Virnau, and M. Kläui, "Real-time observation of topological defect dynamics mediating two-dimensional skyrmion lattice melting," Nat. Nanotechnol. **20**(10), 1405–1411 (2025).
[16] C. Reichhardt, C.J.O. Reichhardt, and M.V. Milošević, "Statics and dynamics of skyrmions interacting with disorder and nanostructures," Rev. Mod. Phys. **94**(3), 035005 (2022).
[17] J. Zázvorka, F. Jakobs, D. Heinze, N. Keil, S. Kromin, S. Jaiswal, K. Litzius, G. Jakob, P. Virnau, D. Pinna, K. Everschor-Sitte, L. Rózsa, A. Donges, U. Nowak, and M. Kläui, "Thermal skyrmion diffusion used in a reshuffler device," Nat. Nanotechnol. **14**(7), 658–661 (2019).
[18] R. Gruber, J. Zázvorka, M.A. Brems, D.R. Rodrigues, T. Dohi, N. Kerber, B. Seng, M. Vafaee, K. Everschor-Sitte, P. Virnau, and M. Kläui, "Skyrmion pinning energetics in thin film systems," Nat. Commun. **13**(1), 3144 (2022).
[19] C. Song, N. Kerber, J. Rothörl, Y. Ge, K. Raab, B. Seng, M.A. Brems, F. Dittrich, R.M. Reeve, J. Wang, Q. Liu, P. Virnau, and M. Kläui, "Commensurability between Element Symmetry and the Number of Skyrmions Governing Skyrmion Diffusion in Confined Geometries," Adv. Func. Mater. **31**(19), 2010739 (2021).
[20] R. Gruber, M.A. Brems, J. Rothörl, T. Sparmann, M. Schmitt, I. Kononenko, F. Kammerbauer, M.-A. Syskaki, O. Farago, P. Virnau, and M. Kläui, "300-Times-Increased Diffusive Skyrmion Dynamics and Effective Pinning Reduction by Periodic Field Excitation," Adv. Mater. **35**(17), 2208922 (2023).
[21] N. Kerber, M. Weißenhofer, K. Raab, K. Litzius, J. Zázvorka, U. Nowak, and M. Kläui, "Anisotropic Skyrmion Diffusion Controlled by Magnetic-Field-Induced Symmetry Breaking," Phys. Rev. Applied **15**(4), 044029 (2021).
[22] F. Rucker, A. Bezvershenko, D. Mettus, A. Bauer, M. Garst, A. Rosch, and C. Pfleiderer, "Shaking and pushing skyrmions: Formation of a non-equilibrium phase with zero critical current," (2025).
[23] J.M. Kosterlitz, and D.J. Thouless, "Long range order and metastability in two dimensional solids and superfluids. (Application of dislocation theory)," J. Phys. C: Solid State Phys. **5**(11), L124 (1972).
[24] J.M. Kosterlitz, and D.J. Thouless, "Ordering, metastability and phase transitions in two-dimensional systems," J. Phys. C: Solid State Phys. **6**(7), 1181–1203 (1973).
[25] B.I. Halperin, and D.R. Nelson, "Theory of Two-Dimensional Melting," Phys. Rev. Lett. **41**(2), 121–124 (1978).
[26] D.R. Nelson, and B.I. Halperin, "Dislocation-mediated melting in two dimensions," Phys. Rev. B **19**(5), 2457–2484 (1979).
[27] A.P. Young, "Melting and the vector Coulomb gas in two dimensions," Phys. Rev. B **19**(4), 1855–1866 (1979).
[28] S.C. Kapfer, and W. Krauth, "Two-Dimensional Melting: From Liquid-Hexatic Coexistence to Continuous Transitions," Phys. Rev. Lett. **114**(3), 035702 (2015).
[29] K. Zahn, R. Lenke, and G. Maret, "Two-Stage Melting of Paramagnetic Colloidal Crystals in Two Dimensions," Phys. Rev. Lett. **82**(13), 2721–2724 (1999).
[30] R. Gruber, J. Rothörl, S.M. Fröhlich, M.A. Brems, T. Sparmann, F. Kammerbauer, M.-A. Syskaki, E.M. Jefremovas, S. Krishnia, A. Sudbø, P. Virnau, and M. Kläui, "Skyrmion Lattice Domain Formation in a Non-Flat Energy Landscape," (2025).
[31] M.A. Brems, T. Sparmann, S.M. Fröhlich, L.-C. Dany, J. Rothörl, F. Kammerbauer, E.M. Jefremovas, O. Farago, M. Kläui, and P. Virnau, "Realizing Quantitative Quasiparticle Modeling of Skyrmion Dynamics in Arbitrary Potentials," Phys. Rev. Lett. **134**(4), 046701 (2025).

[32] A.A. Thiele, "Steady-State Motion of Magnetic Domains," Phys. Rev. Lett. **30**(6), 230–233 (1972).
[33] J.A. Anderson, J. Glaser, and S.C. Glotzer, "HOOMD-blue: A Python package for high-performance molecular dynamics and hard particle Monte Carlo simulations," Comput. Mater. Sci. **173**, 109363 (2020).
[34] D.B. Allan, T. Caswell, N.C. Keim, C.M. van der Wel, and R.W. Verweij, "soft-matter/trackpy: v0.6.4," (2024).
[35] J.L. Finney, and J.D. Bernal, "Random packings and the structure of simple liquids. I. The geometry of random close packing," Proc. R. Soc. A **319**(1539), 479–493 (1997).
[36] Y. Ge, J. Rothörl, M.A. Brems, N. Kerber, R. Gruber, T. Dohi, M. Kläui, and P. Virnau, "Constructing coarse-grained skyrmion potentials from experimental data with Iterative Boltzmann Inversion," Commun. Phys. **6**(1), 1–6 (2023).
[37] R. Gruber, J. Rothörl, S.M. Fröhlich, M.A. Brems, F. Kammerbauer, M.-A. Syskaki, E.M. Jefremovas, S. Krishnia, A. Sudbø, P. Virnau, and M. Kläui, "Source Data - Skyrmion Lattice Order Controlled by Confinement Geometry," (2025).